EnE-HVAC

Energy Efficient Heat Exchangers for HVAC Applications

Grant Agreement number:	**314648**
Project acronym:	**EnE-HVAC**
Project title:	**Energy Efficient Heat Exchangers for HVAC Applications**
Funding Scheme:	**FP7-NMP**
Deliverable number:	**D4.1**
Date:	**28/2 2014**
Coordinator:	**Dr. Mikael Poulsen, Danish Technological Institute**
Project website address:	**http://www.ene-hvac.eu**

Contents

Energy Efficient Heat Exchangers for HVAC Applications
Project No: 314648 – EnE-HVAC
Report on D4.1: Proof-of-concept

2

Abstract and conclusion

The objective of this work package is to scale up the technologies developed in WP1, WP2, and WP3 from laboratory technologies to industrial scale use. Specifically, the work covered in this deliverable report is the scale-up process of the nanotechnological coating technologies developed and tested in small scale in this project.

As described in previous deliverable report, a selection of surface modifications have been made for the improvement of heat transfer capabilities. This report describes some of the considerations regarding scaling of these technologies to provide a proof-of-concept of the scalability.

In short, the following work has been conducted to achieve proof-of-concept:

- Development and testing of processes for up scaling the sol-gel technology to be applied on heat exchanger plates. This includes:
    - Development of equipment for coating heat exchanger plates
    - Calculation of price of production (in laboratory scale) of coated heat exchanger plates. These calculations will most likely be a part of the important parameters when finally selecting coatings for demonstration. If multiple coatings have similar behaviour, this can be a deciding factor for the industrial partners.
- Heat exchanger plates have been coated at Tekniker for validation tests, and the heat exchangers are currently being assembled at Vahterus
- Development and testing of processes for up scaling technologies for nanostructuring heat exchanger plates, including:
    - Development of Colloid deposition procedures to obtain deposition masks on heat exchanger plates
    - Development of physical vapour deposition parameters for obtaining the correct PVD coatings on the heat exchanger plates
    - Calculations on cost-of-production, indicating the final cost for producing heat exchangers using these techniques
- Heat exchanger plates have been structured at DTI for assembly at Vahterus and use in the validation process.

Introduction

Objectives

The objectives of this part of Work Package 4 is to provide a proof-of-concept on the transfer of the nanotechnologies developed through the development work packages WP1-3.

Through WP4, the technologies developed on small scale heat exchangers will be scaled up and implemented on industrial scale heat exchangers in tight corporation with the involved research and industrial partners. The scale up in WP4 will partly serve as proof-of-concept of the scalability of the chosen technologies, but will also provide valuable results on large-scale heat exchanger systems for the following demonstration work package (WP5).

This report will cover the parts involved with scaling the nanotechnological coating system for large-scale heat exchangers, and thus document proof-of-concept of the scalability of these.

Anti-ice surfaces

Introduction

Aim

Anti-ice surfaces shall reduce the energy, today used to avoid or remove (=defrost) ice formation or frost from two different types of heat exchanger surfaces. The first is the air-side of evaporators on heat pumps using ambient air as heat source. The second is the surfaces in contact with the outgoing air of heat-recovery-ventilation systems. There are two different mechanisms, by which a surface can provide anti-ice properties. The first is to avoid (depress) frost formation. Even at subzero temperatures, liquid water condenses on the surface. The drainage of the liquid water should also be improved. The second alternative is to reduce the adhesion of frost. Frost formation is here accepted, but the frost is so easy to remove that no thermal defrosting is necessary. For the latter, a combination with mechanical aids such as vibration was proposed in the project proposal.

Proof of concept

The present work provides a proof of concept for both of the mentioned anti-ice strategies based on laboratory test methods. To investigate freeze-depression, we constructed and built a freezing test chamber, see Figure 1.

Figure 1: left: Freezing test chamber, on the left side, the sample plate (metallic blue) is mounted with a cooling block behind (not visible). right: Image from the camera mounted inside the test chamber. Frost on a bare Al-plate

While various surfaces, when cooled at a rate of 0.1 °C/min, was observed to depress the freezing down to temperatures between -5 and -11 °C before frost occurred on the first spot, it became obvious, that only hydrophobic surfaces are suitable freeze- depression surfaces. Only these show additional depression of the spreading of frost from the spot of first occurrence to the rest of the surface. More specifically, for a smooth surface, a low frost spreading rate and a good drainage of liquid water require high receding water contact angles and a low contact angle hysteresis. The test showed several smooth hydrophobic surfaces, including technical silicone rubber; sol-gel coatings based on silicone additives by DTI, and a sol-gel coating based perfluoroalkylsilanes by TEK providing high receding contact angles resulting in low frost spreading rates. To test frost spreading, the surfaces were wetted by condensation until drops started to run down and subsequently cooled down as described above until the first occurrence of frost was observed. The surfaces were then held at that temperature for about 30 min. The surface area below 0 °C is about 9 x 13,5 cm. For samples with low frost spreading, 40-75% of that area are still ice free after the test. Even though further improvement is desired, the present candidates are already interesting candidates for industrial applications.

The facilitation of ice removal by mechanical aid was successfully demonstrated in a lab test with meshes mounted in front of an industrial scale heat exchanger. Under weather conditions resembling fog at subzero temperatures, frost forms mainly on these meshes keeping the heat exchanger behind almost frost free. With sufficient vibration, the ice is removed from the meshes even without a coating on the meshes, see Figure 2.

Energy Efficient Heat Exchangers for HVAC Applications   *5*
Project No: 314648 – EnE-HVAC
Report on D4.1: Proof-of-concept

Figure 2: Left side: Heat exchanger with meshes, frost free after vibration by a beat mill. Right side: Frost blocking an otherwise identical heat exchanger without meshes.

The application of coatings to facilitate mechanical ice removal was in agreement with the industrial partners not investigated. The implementation of this technique was expected to be too complicated and too costly. The ice adhesion performance of the various surfaces was indirectly determined by receding contact angle measurements pointing exactly towards the same candidates as mentioned above for slow frost spreading, with measured receding water contact angles of 89 to 94°.

Sol-gels for anti-ice surfaces

Deliverable D1.2 of WP1 already provides both background and results of the different materials in detail. Due to the proof of concept in WP4 being based on laboratory tests, there is a very strong interconnection with WP1. Thus, the content of D1.2 is not repeated herein in all detail. As an update to D1.2, DTI determined advancing and receding contact angles of all smooth TEK coatings (see

Table 2). This led to a further promising candidate for freeze-depression and slow frost spreading. TEK's composition 3 provides a significantly higher receding water contact angle than all other coatings developed by TEK and was thus investigated in the freezing test chamber as described in the introduction at a cooling rate of 0.1 °C/min. The temperature for the first occurrence of frost was -9,7 °C, the frost spreading rate is as low as well. Comp. 3 performs on the same level as DTI's coating 01 or the commercial silicone rubber by Nusil.

Coating development by TEK

The objective of this part is the development of superhydrophobic and hydrophobic films by the sol-gel process towards avoiding icing process onto aluminum surfaces.

As explained in deliverables D1.2 and D2.3, the sol-gel process is a chemical synthesis technique for preparing coatings, gels, glasses, and ceramic powders. Compared to other surface modification techniques, sol-gel is a simple, economic and effective method to produce high quality coatings. In addition, sol- gel has several advantages including low cost, high adherence to the surface, chemical stability, film uniformity and low sintering temperature. This process involves hydrolysis and condensation reactions of metal alkoxides or organosilanes and optional organic precursors to give gels (Figure 3).

Hydrolysis reaction:
$$Si(OC_2H_5)_4 + 4H_2O \rightarrow Si(OH)_4 + 4C_2H_5OH$$

Condensation of water:
$$nSi(OH)_4 \rightarrow nSiO_2 + 2nH_2O$$

Condensation of alcohol:
$$Si(OH)_4 + Si(OC_2H_5)_4 \rightarrow 2SiO_2 + 4C_2H_5OH$$
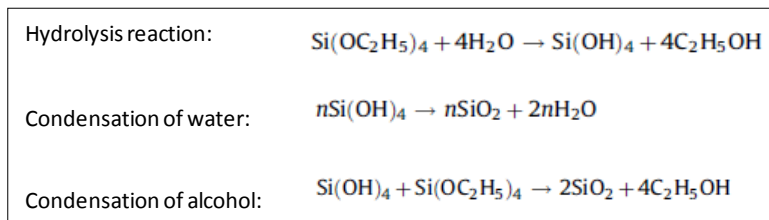
Figure 3: Hydrolysis and condensation reaction of the sol- gel process.

They are applied by standard methods such as spray-coating, dip-coating or spin-coating and are widely used due to their excellent adhesion to other materials such as metals and their high chemical and wear resistance. Typical film thicknesses obtained varies between a few nm to a few µm, which makes them extremely interesting for the enhancement of heat exchangers, where good heat transfer capabilities are required in combination with other properties such as low adhesion of ice, improved bubble formation, antifouling, etc.

Sol gel technology can be structured by the following steps, each step needs to be optimized, and several parameters need to be controlled (Figure 4).

Energy Efficient Heat Exchangers for HVAC Applications   *7*
Project No: 314648 – EnE-HVAC
Report on D4.1: Proof-of-concept
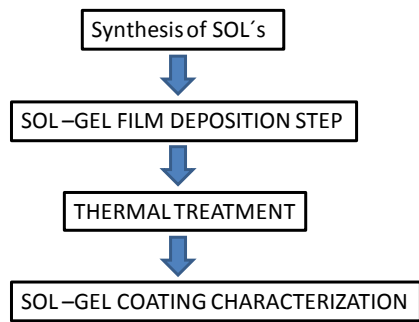
Figure 4: Steps of the sol-gel route.

In order to obtain superhydrophobic, hydrophobic and hydrophilic coatings, TEK has followed three synthesis strategies (Figure 5), previous reported in D1.2:
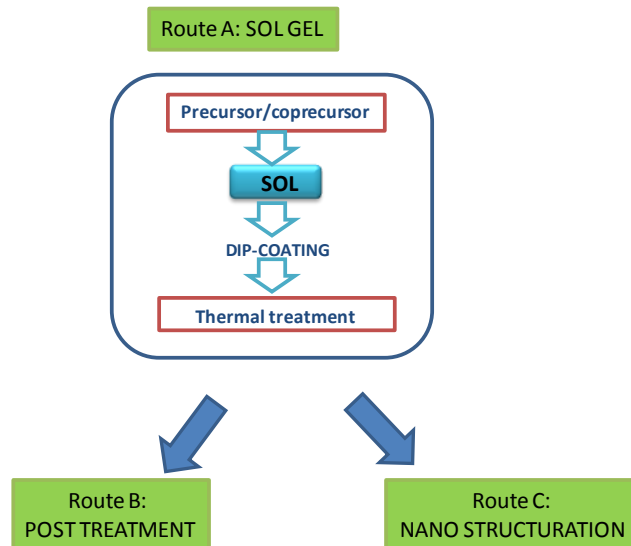
Figure 5: TEK's routes of synthesis for superhydrophobic, hydrophobic and hydrophilic coatings.

A) Sol-gel route: Hydrophobic or hydrophilic coatings

Following this synthesis route, coatings with superhydrophobic, hydrophobic or/and hydrophilic properties have been prepared, as mentioned earlier, it has been necessary to optimize all the steps involved in the sol gel process: Co-precursor nature, sol gel stability, and deposition conditions in the dip coating step.

Sols has been prepared using TEOS as precursor, and several co-precursors such us iso-BTMS, HDTMS, Trichloro-(1H,1H,2H,2H-perfluorooctyl)-silane (TPFOS), 1H,1H,2H,2H-Perfluoro-decyl-triethoxysilane (PFDTS) and 1H,1H,2H,2H-Perfluoro-octyl-triethoxysilane (PFOTS) in different molar ratios, as hydrophobic agents. Different Energy Efficient Heat Exchangers for HVAC Applications Project No: 314648 – EnE-HVAC Report on

Energy Efficient Heat Exchangers for HVAC Applications   *8*
Project No: 314648 – EnE-HVAC
Report on D4.1: Proof-of-concept

D2.3: First generation coatings types and molar ratios of solvent (methanol and ethanol) have been used for the optimization of the process too.

The coatings have been deposited using dip coating equipment testing different immersion rates (300, 500 and 700 mm/s). Finally, the coating curing step has been tested with different thermal treatments, from 150 to 250° C and from 1 to 24 hours.

B) Post-treatment route: Superhydrophobic coatings

Combining the sol-gel route with a post-treatment process using a hydrophobic agent allows to improve the hydrophobicity properties of the coatings. The post-treatment process consists of immersing the coatings into a solution containing a hydrophobic agent.

Once optimized coatings by sol-gel route A were prepared, different types of post-treatment have been optimized controlling the same parameters.

C) Nanostructuration route: Superhydrophobic coatings

The sol-gel route is combined with a nanostructuration process in order to increase the hydrophobicity of the coatings. The nanostructuration process can be performed either directly with the coating or indirectly by structuring the substrate and depositing a coating onto the structured substrate. Different techniques of nanostructuration can be selected (Figure 6).
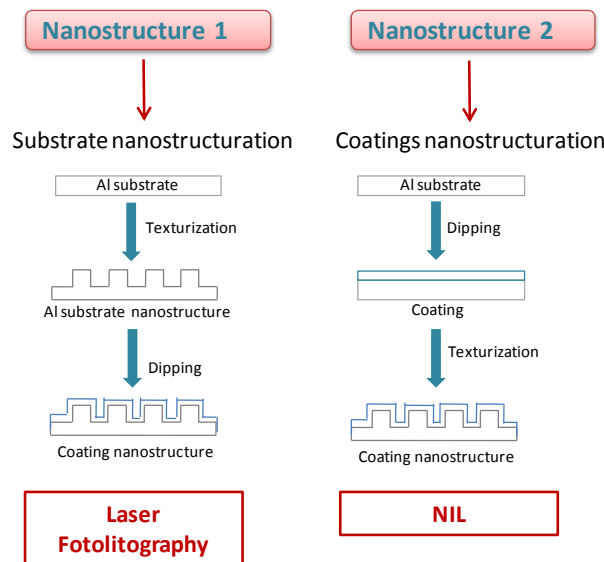
Figure 6: Different techniques of nanostructuration of sol-gel coatings

Each process has been optimized and different parameters and variables have been controlled, as a function of each process.

Summary of Characterization of Sol-gel coatings

Coatings from strategy A and B

Table 1 shows the best results obtained for the different compositions of sol- gel coatings obtained by route A and route B in WP1. Table X1 shows all advancing and receding contact angles measured in WP1 for both TEK, DTI and commercial reference coatings.

Table 1: Contact angles of the best results of sol-gel coatings prepared by route A and B. The coatings with references 4, 6, 7, 9 and 10 were investigated in the freezing test chamber by DTI.

					Substrate	
					Al Lab	Al real plane
Route	Properties	Reference	Co-precursor/Post. Agent	Thermal treatment	C.A.	C.A.
Route A	Hydrophobic	1	BTMS	150°C/ 5h	103	99
		2	HDTMS	150°C/ 1h	100	92
		3	PFOTS	150°C/ 1h	97	98
	Hydrophilic	5	BTMS	250°C/24h	3	7
		6	HDTMS	250°C/24h	3	8
Route B	Superhydrophobic	4	HMDZ	150°C/ 1h	109	107
		7	PFOTS		108	108
		8	PFDTS		113	114
		9	HMDZ		109	115
		10	PFOTS		117	124
		11	PFDTS		114	123

Energy Efficient Heat Exchangers for HVAC Applications   *11*
Project No: 314648 – EnE-HVAC
Report on D4.1: Proof-of-concept

Table 2: Advancing and receding water contact angles of both TEK; DTI and reference samples. Dc is the critical droplet diameter for droplets to start sliding down a vertical surface, calculated according [Kim2012: P. Kim, T-S. Wong, J. Alvarenga, M.J. Kreder, W.E. Adorno-Martinez, J. Aizenberg; ACSNano 6 (8) (2012), 6569.]. According to [same lit.] a low Dc provides slow ice spreading

Sample	DTI Plate no	Used/new *)	θstatic (DTI) / °	θadv / °	θrec / °	Dc	Θstatic from TEK / °
Metal references							
Al from Q-Lab	-	New	92,6±1,5	92,4±2,5	55,8±3,1		
Carbon steel from Q-Lab		New	75,3±0,65	68,7±1,4	26,2±1,2	5,0 mm	
Electro-pol. SAE 316 steel	-	Used	78,1±5,2	72,0±3,4	38,0±4,8	4,5 mm	
	-	New	72,5±2,1	71,0±8,2	37,2±7,0	4,6 mm	
Polymer references							
Polypropylene (PP) foil	-	Used	87,1±2,3	88,5±3,7	60,6±6,8	3,7 mm	
FEP (fluorina-ted eth. prop.)		Used	106,4±1,2	111,5±2,9	86,3±6,5	2,5 mm	
Nusil R 2810 (silicone rub.)	-	New	100,8±0,4	103,4±2,1	90,6±1,9	2,0 mm	
	#32	Used	111,8±0,3	115,4±2,2	89,0±1,0	2,4 mm	

DTI coatings							
DTI Coat. 01 on CS	#9	Used	104,7±0,7	104,3±1,6	93,6±1,4	1,8 mm	
	-	New	105,4±0,7	103,5±0,9	96,2±1,8	1,6 mm	
	#7	Used	105,4±0,8	101,4±1,5	94,5±1,6	1,6 mm	
DTI Coat. 01 on LUVE Al	#19	Used	104,2±0,6				
	#23	Used	105,2±0,5				
DTI Coat. 01 on Q-Lab Al	-	New	104,6±0,6	106,2±0,8	95,8±1,5		
DTI Coat. 02 on CS	#14	Used	85,1±0,9	85,1±0,9	66,5±2,1	3,2 mm	
	-	New	87,3±0,8	87,2±1,4	71,4±2,3	2,8 mm	
	QLab Al	New	87,6±1,0	88,8±1,8	72,9±0,7		
DTI Coat. 03 on CS	#25	Used	108,0±0,5	107,4±1,5	90,1±0,2	2,2 mm	
	#24	Used	107,6±0,3	107,1±1,1	90,3±0,7	2,2 mm	
	-	New	108,0±0,4	108,8±0,7	89,8±0,4	2,3 mm	
DTI C. 04 on CS (silicone rub.)	-	New	108,6±2,6	111,6±3,6	93,4±0,9	2,1 mm	
	#26	Used	111,4±0,9	107,5±2,9	91,4±0,9	2,2 mm	
	-	New	110,0±0,5	105±2,1	88,7±1,0	1,9 mm	
DTI C. 05 on CS (ice nucleating)	-	New	101,1±0,4	101,9±3,7	88,7±1,0	2,1 mm	
	#29	Used	101,0±0,3	98,1±3,3	87,6±1,5	2,0 mm	

TEK coatings on LUVE-Al (also named "Al real plane" in this report) Comp. no. is identical with the reference no. used in the tables describing the TEK coatings							
TEK Comp.1	-	New	106,9±4,2	107,2±4,4	45,6±4,6	4,1 mm	
TEK Comp.2	-	New	110,7±2,0	112,5±2,2	30,3±3,6	4,2 mm	
TEK Comp.3	-	New	107,0±0,8	105,1±1,4	94,9±1,0	1,8 mm	
TEK Comp.4	#11	Used	105,0±1,1	111,8±4,4	52,8±1,6	3,8 mm	107
TEK Comp.5	-	New	28,4±4,3	-	-	-	
TEKComp.6	#12	Used	>10	>10	>10	-	8
	#22	Used					8
TEK Comp.7	#13	Used	105,0±2,1	113,2±2,8	45,6±1,9	3,9 mm	108
TEK Comp.8	-	New	112,0±2,7	110,1±5,8	53,5±4,1	3,8 mm	
TEK Comp.9	#17	Used	120,8±1,1	132,1±4,0	51,1±2,5	2,8 mm	115
TEK Comp.10	#16	Used	105,5±2,7	111,6±5,4	42,0±2,0	4,1 mm	124
TEK Comp.11	-	New	106,9±4,2	132,1±2,7	62,2±2,1	2,7 mm	
Preliminary TEK coatings on Q-Lab Al							
TEK Pre 0.1		New	105,6±1,9	113,1±2,8	21±1,4		113,5
TEK Pre 1.1		New	5,3±0,8	10,8±2,1	>10		3,2

*) "Used" means that the plates have been used in a freezing test prior to contact angle measurements. This would make a difference in case of coating degrades.

Preliminary studies of the icing performance in the freezing test chamber at DTI show that for the TEK coatings, like for all other investigated coatings, the freezing temperature is in the same range as for the bare metal references. However, the spreading of frost from the spot of first occurrence is strongly delayed by composition 3, which also provides the highest receding contact angle. The other investigated hydrophobic surfaces comp. 4, 7, 9 and 10 also provide slower frost spreading, but the effect is much weaker as for best systems:TEK comp. 3, DTI's coating 01 and Nusil silicone rubber. TEK will continue with the optimization process of scale- up, and focus our work on the optimization of nanostructured surfaces.

Coatings from strategy C

To optimize the nanostructuring process, it was necessary to select one of the composition of strategy A and B. Composition 1 was selected to improve the hydrophobic properties, as this is the most cost-effective and easily prepared composition showing a good hydrophobic behavior with high average value of static contact angle.

Table 3 and Table 4 summarizes the C.A. characterization of coatings and substrates nanostructured by laser and photolithography, respectively.

Table 3: Static water contact angle (C.A.) measurements of sol-gel coatings onto Al nanostructured by laser.

Process	Geometry	CA substrate nanostructured	CA substrate nanostructured + coating (composition 1)	Selection TEK
	C.A. of Al substrate	84.42	113.1	
Laser	Pyramids 1	69.8	134.9	
	Pyramids 2	68.0	140.1	√
	Pyramids 3	61.4	133.1	
	Pyramids 4	14.48	143.6	√
	Pyramids 5	----	----	
	Pyramids 6	----	----	
	Pyramids 7	100.4	112.0	
	Pyramids 8	----	----	
	Pyramids 9	----	----	
	Channels 1	51.4	136.7	
	Channels 2	41.6	135.5	
	Channels 3	40.7	138.2	
	Channels 4	33.3	141.0	√
	Channels 5	24.4	140.1	√
	Channels 6	11.7	142.1	√
	Channels 7	110.6	116.1	
	Channels 8 (2)	110.5	115.8	
	Channels 9 (3)	116.2	116.0	
	Channels 10 (4)	107.2	111.3	
	Channels 11 (5)	129.7	126.5	

Table 4: Static water contact angle (CA) measurements of sol-gel coatings onto Al nanostructured by photolithography.

Process	Geometry	CA substrate nanostructured	CA substrate nanostructured + coating (composition 1)	Selection TEK
Photolithography	Holes 80 μm, deep 1.5 μm	67.7	117.4	
	Holes 80 μm, deep 2.5 μm	98.2	115.7	√
	Holes 80 μm, deep 3.5 μm	74.5	114.8	
	Holes 80 μm, deep 5.7 μm	73.0	119.6	
	Holes 300 μm, deep 4.5-8.7 μm	78.77	102.1	
	Pillars 500x500 μm, deep 1 μm	82.0	111.7	√
	Pillars 500x500 μm, deep 2 μm	83.8	112.3	
	Pillars 500x500 μm, deep 3.5 μm	76.2	105.1	
	Pillars 500x500 μm, deep 3.8 μm	81.31	108.0	

A preliminary selection of the best coatings was made by TEK based on considerations of homomogeneity, adherence, perfect coverage of substrates and high static contact angle measurements.

These nanostructures were selected to continue with the scale-up process to bigger sizes as minimum of 10 x 15 cm. These samples will be evaluated as anti-icing coatings characterized them in real conditions in the freezing chamber at DTI.

Evaporation heat transfer

Introduction

When improving heat exchanger efficiencies of evaporators and condensers, it is important to look at how the boiling behavior of these systems can be optimized in order to give a decreased energy consumption. Looking at a schematics of the heat exchanger system (see Figure 7 below), where the coolant is evaporated on the left hand side, and condensed again on the right hand side, the efficiency (ε) is strongly dependent on the difference between the evaporation temperature (T_0) and the condensation temperature (T_c).
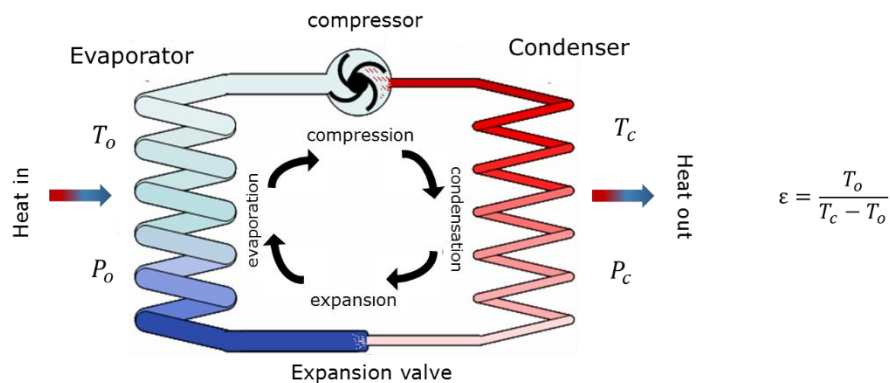
Figure 7: schematics of a heat exchanger system

As is illustrated in the figure above, the evaporation process in the evaporator of an air-conditioning unit or a heat pump occurs as flow boiling due to the presence of forced convection. Boiling in the absence of forced convection, known as pool boiling, can serve as a model to comprehensively illustrate the correlation between the surface superheat (known as the wall superheat) and the heat flux as flow boiling and pool boiling show comparable effects.

Wanting to maximize the efficiency of the heat exchanger system, increasing the evaporation temperature is one very viable approach. This increase in evaporation temperature can be achieved if the boiling efficiency is enhanced.

Looking at the evaporation temperature, then this is dependent on the flux transferred through the heat exchanger surface and the Heat transfer coefficient, thus q = α ($T_{surface}$ – T_0), where q is the flux, α the heat transfer coefficient, $T_{surface}$ the temperature of the heat exchanger surface, and T_0 the evaporation temperature. The difference between the wall and coolant temperature ($T_{surface}$ – T_0) is known as the wall superheat and is denominated ΔT. The heat flow rate per area (i.e. Q/A) is known as the heat flux. To achieve a high heat transfer coefficient one needs a surface that shows a high heat flow rate at small wall superheat values.

Energy Efficient Heat Exchangers for HVAC Applications   *17*
Project No: 314648 – EnE-HVAC
Report on D4.1: Proof-of-concept

A normal boiling curve for water in pool boiling takes the form as illustrated in Figure 8 (left), where the mechanisms of boiling can be separated into several regimes. In the early phase (low wall superheat, ΔT), there is a regime with natural convection only, during this phase, only a small amount of heat is transferred across the surface. At a certain dT bubbles start forming (A) and increasing dT leads to fully developed nucleate boiling (B). At a certain dT (C) a film of gas starts forming on the surface, and the critical heat flux (CHF) is reached, followed by a transition to fully developed film boiling (D).

The regime having the most effective heat transfer across the surface is the nucleate boiling regime. In order to create more efficient heat exchangers, surfaces with an earlier onset of bubble boiling can be developed, thus enabling a higher flux at a certain dT (see Figure 8– right)
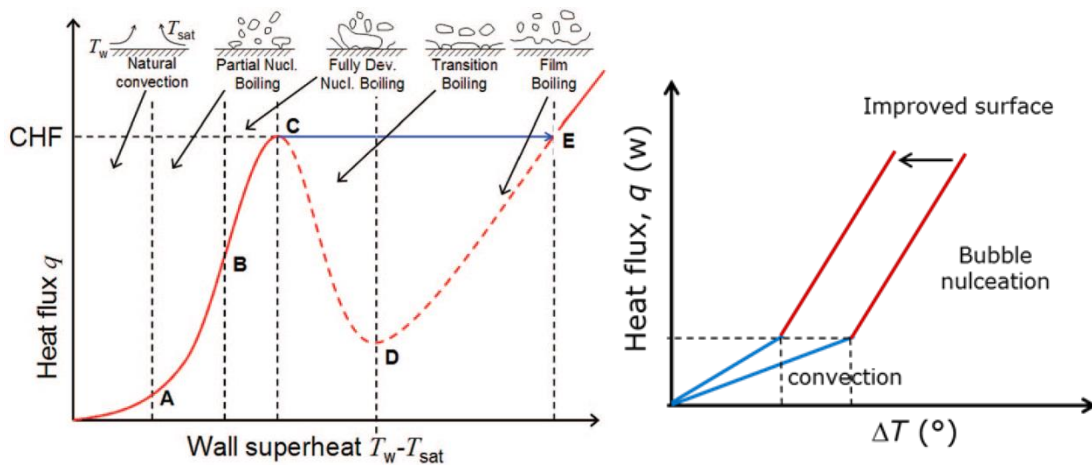
Figure 8: Left: Pool boiling regimes; Right: effect of early onset of bubble nucleation

Deliverable report for D2.2 considers the development of nanostructured coatings and Sol-gel coatings for improvement of heat transfer. In that report (D2.2), consideration on the choice of coatings for up scaling is also presented in some detail. The focus in the current report will be on the up-scaling process.

Energy Efficient Heat Exchangers for HVAC Applications   *18*
Project No: 314648 – EnE-HVAC
Report on D4.1: Proof-of-concept

Scaling surface technologies

Sol-gel coatings for anti-ice surfaces

As previously mentioned for anti ice surfaces based on sol gel coatings, experimental results do not show good behavior or improvement of anti-ice properties. Therefore, surface nanostructuring was selected as a strategy to continue with the scale-up process to bigger sizes as minimum of 10 x 15 cm.

Figure 9 show the varieties techniques used to nanostructure the surfaces.

Figure 9: Photolithography, NIL, picoseconds and nanoseconds laser.

Energy Efficient Heat Exchangers for HVAC Applications   *19*
Project No: 314648 – EnE-HVAC
Report on D4.1: Proof-of-concept

There are important differences between these techniques for creating nanostructures, these could determine viability, simplicity and the final cost of scale-up of the process in order to reach the final objective. The table below (Table 5) summarizes the main advantages, disadvantages, along with time and costs considerations for the different processes.

Table 5: Description of different nanostructuration techniques

Nanostructuration technique	Specifications	Advantages	Disadvantages	Process time	Added cost	Scale-up viability
Laser	Picoseconds	3D-microstructuring. Variety of geometries. Any type of material (metals, polymers, ceramics, glass, wood). Direct process. High precision. High speed.	High speed is limited to areas inside the scanner field (30-50 mm²). Large areas: slower speed (v = 200 mm/s).	~ 2h	----	√
	Nanoseconds	Applications like metal and plastic. Laser by optical fiber. Portable equipment.	Higher thermal effect.	~ 20min	----	√
Photolithography	With Al etching	Microstructuration (1-2 µm). More cheaper	Mask can be damaged by wafer contact. Limited to size of substrates, not for curved substrates	~ 30min (exposure + wet etching)	Al wet etching	√
Nanoimprint lithography (NIL)	Stamp of 1x1 cm	Micro and nanostructuration with high resolution.	Size of substrates, area of nanostructures, not for curved substrates	~ 3h	Expensive	X

To optimize the nanostructuring process, it was necessary to select one of the compositions from strategy A and B. Composition 1 was selected to improve the hydrophobic properties, as the cheapest and easily composition showing a good hydrophobic behavior with high average value of static contact angle. Table 6 summarizes the main nanostructures selected by different techniques and different geometries and parameters.

Table 6: Parameters and geometries selected of nanostructuration process.

Nanostructuration technique		Geometry	Parameters
Laser	picoseconds	Pyramids	w = d = 70 um, dp = 15 um
			w = d = 150 um, dp = 60 um
		Channels	w = 43 um, d = 11 um, dp = 4 um
			w = 45 um, d = 11 um, dp = 20 um
	nanoseconds	Craters	d= 80µm, φ=60 µm, dp=30 µm
		Grid Lines	d=75µm, φ=48µm, dp=10 µm
Photolithography		Holes	Φ= 80µm, dp=2.5µm
		Pillars	500x500µm, dp=1 µm

The nanostructuring process of each structure including the complete topographic characterization of the samples is in progress. It is necessary to check the homogeneity of the nanostructure, the adherence and coverage of the coating on the substrate by Scanning Electron Microscopy (SEM), Atomic Force microscopy (AFM), Confocal Laser Microscopy (CLM) and static contact angle (CA) measurements, and the superhydrophobicity by higher static contact angle measurements.

The Figure 10shows photography of a real nanostructure using a picoseconds laser and scale-up to 10 x 15 cm Al substrate and the complete characterization by different microscopic techniques.
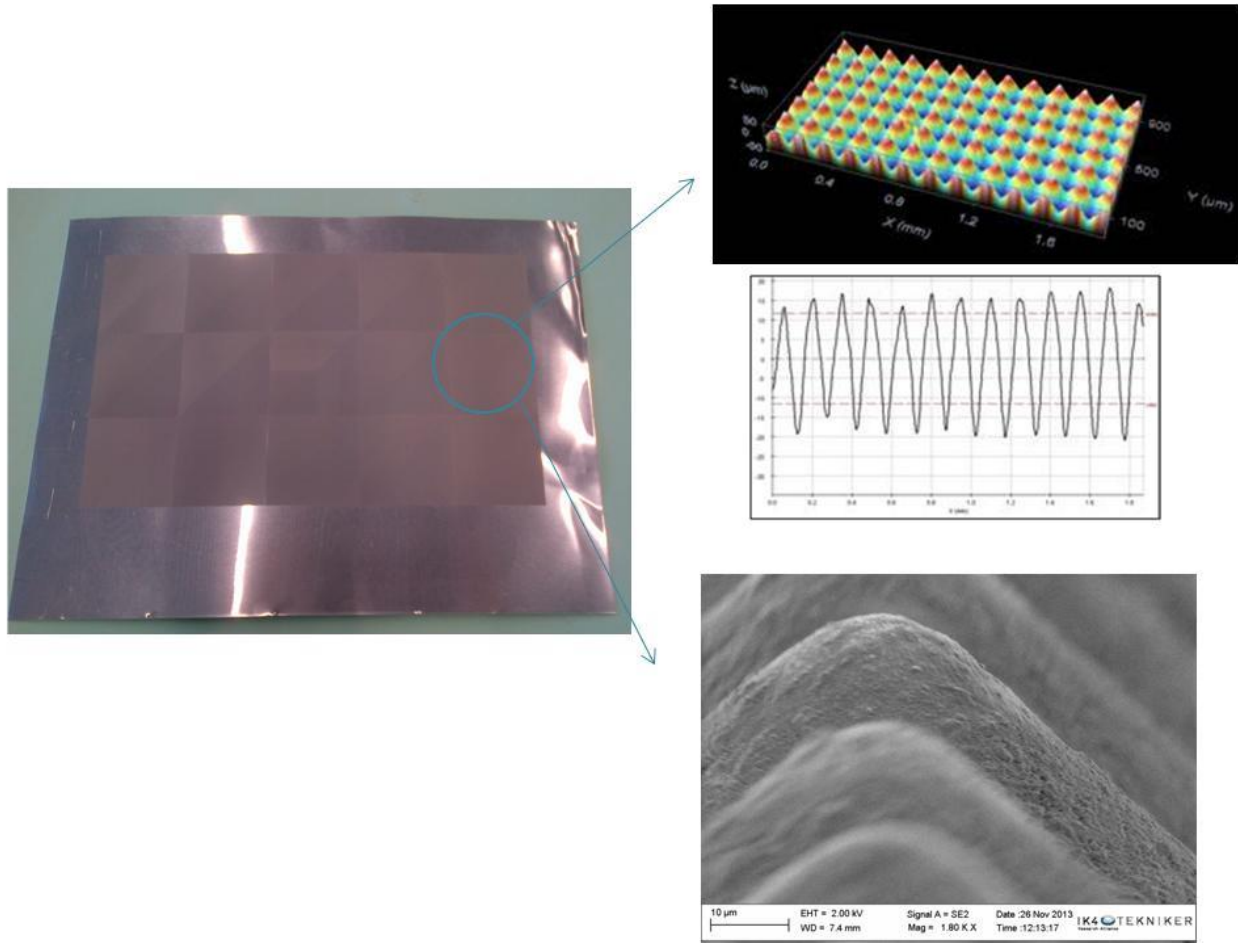
Figure 10: Real Al substrate nanostructure by picoseconds laser with pyramids structure, real photography and microcopy characterization.

In order to complete the characterization and evaluate the anti-icing properties, these samples will be evaluated under real conditions at the freezing chamber setup at DTI when they are ready.

Selection of the final substrates for scale-up onto industrial scale heat exchangers will be based partially on performance measurement, but also on scalability of the sol-gel process.

Structured surfaces via Colloidal lithography

Two different techniques (electro deposition and spray deposition) for performing colloidal lithography on large area surfaces have previously been investigated. Deliverable report *2.2. First Generation Surfaces* reported on the results and the pros and cons of the two methods. Electro deposition produced particle patterns with good control over the particle coverage and no multilayer formation. However, it was deemed unfit for the large-scale production needed for the heat exchangers in this project. It would have been technically feasible but it would have required a relatively complex electrode setup to perform electro deposition on the large and corrugated heat exchanger plates. Thus, spray deposition of the particles was selected as the method to structure the plates.

500 nm polystyrene particles were chosen for the patterning because small-scale heat transfer experiments on the test cell at DTI showed promising heat transfer characteristics for surfaces with this size of features. Tests in both CO_2 and NH_3 showed enhanced heat transfer capabilities (pool boiling commenced at a lower wall superheat temperature compared to unstructured surfaces) for the structured surfaces with 500 nm features. Deliverable report *2.2. First Generation Surfaces* provides the background and results for these small-scale experiments on colloidal lithography structured surfaces of different feature sizes.

The spray deposition of particles was tested on small stainless steel substrates and the resulting particle patterns were investigated visually and using scanning electron microscopy (SEM). Originally, the particles were sprayed onto substrates that were placed in a hot oven but due to size limitations (not enough room to deposit particles on the heat exchanger plates in the oven) the heating of the substrate was abandoned and the substrates were kept at room temperature.
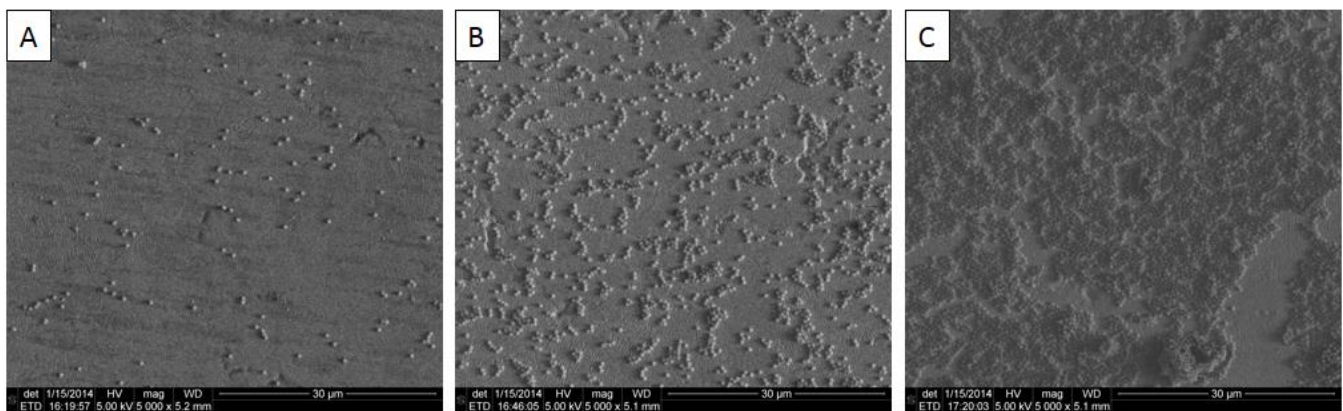
Figure 11: Scanning electron microscope images of three spray deposited colloidal lithography samples prepared at room temperature. Varying the particle concentration and/or distance between the airbrush nozzle and sample can lead to particle coverage on the surface that are: too low (A) almost adequate (B) or too high (C). Some agglomeration is present in all samples but it increases with increasing surface coverage. Particle solution concentrations: A = 5%, B = 5%, C = 7.5%.
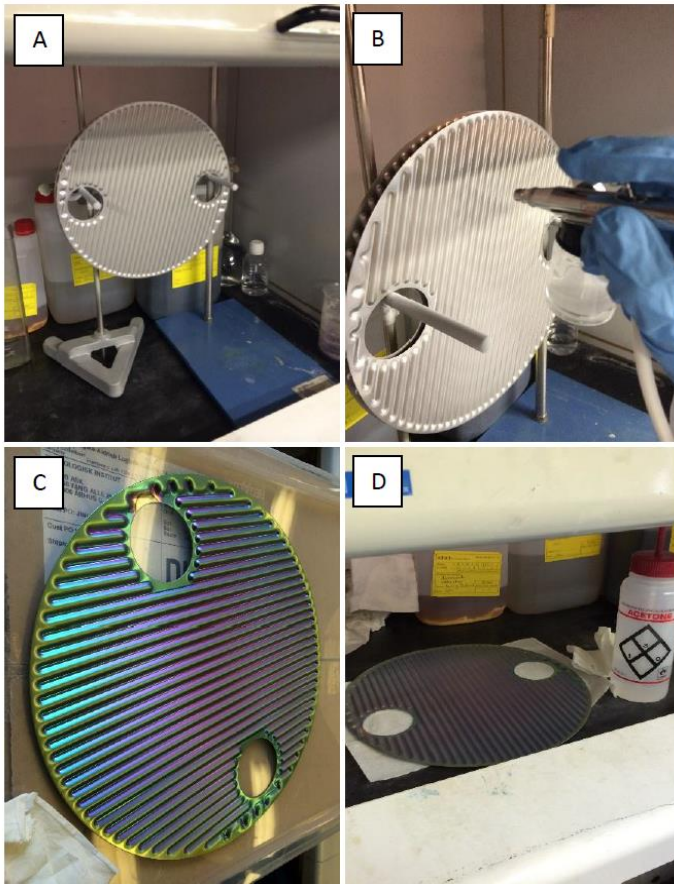
Figure 12: Nano structuring of heat exchanger plates. A: Mount for plates during colloidal lithography. B: Spraying particles onto the plates. C: After PVD deposition of TiO2 onto the nanostructured plates. D: removal of particles using a combination of mechanical removal and acetone wipe.

Two parameters of key importance for successful particle deposition in the spray deposition process are the particle concentration and the distance between the nozzle of the airbrush and the substrate. The particle concentration should be in the range where there is just one particle per drop of solvent in the spray mist. If there are more particles in each drop, the particles will aggregate during solvent evaporation. The distance between the nozzle and the substrate also affects the particle coverage. If the nozzle is too far from the substrate, no or very few particles will reach the substrate. On the other hand, if the nozzle of the airbrush is too close many particles will land on the substrate, but the acetone will not have time to evaporate and hence the substrate becomes wet and the risk of large particle aggregates is highly increased.

Tests were performed on small stainless steel substrates that were inspected by eye during and after spray deposition to see whether the substrate was wet and whether a white tinge (originating from an adequate polystyrene particle layer) appeared on the substrates after deposition. Different particle concentrations were also tested and visually inspected and some samples were inspected in the scanning electron microscope. SEM images of particles on stainless steel test substrates are shown in Figure 11. The samples in image A and B were made with the same particle concentration (5% particle solution to 95% acetone) but differences in spraying distance has resulted in very different surface coverage. This illustrates the importance of the spraying distance.

The heat exchanger plates were coated in a fashion very similar to the small samples. The airbrush was kept at approximately the same distance to the substrate and a steady stream of acetone/particle mist was applied while moving the airbrush slowly back and forth. Every time the edge was reached the airbrush was moved far enough out over the edge so no particles could land on the plate and then the airbrush was moved one step down. The mounting of a heat exchanger plate, ready for particle deposition, inside a fume hood is shown in the photograph in Figure 12A. The spray deposition is shown in Figure 12B. After particle deposition, the plates

Figure 13: A coated heat exchanger plate is taken out of the PVD deposition chamber. Four plates can be coated in one batch.

were coated with a thin film of TiO_2 (a coated plate is shown in Figure 12C) and the particles were removed mechanically by rubbing with paper towels and chemically by wiping with acetone (Figure 12D).

More information on the coating process can be found in deliverable report *2.2. First Generation Surfaces*. In brief, the coatings are deposited by magnetron sputtering, a type of physical vapor deposition (PVD) technique. Care was taken not to elevate the substrate temperature above the glass transition temperature of the polystyrene particles and the normal etching phase was omitted as this, just as rising the temperature above the glass transition temperature, can melt and deform the particles. Thickness optimization and homogeneity tests were performed and results are presented in deliverable report 2.2. A photo of a coated heat exchanger plate being taken out of the PVD chamber is shown in Figure 13.

40 Vahterus heat exchanger plates have been patterned with polystyrene particles through spray deposition and subsequently coated with PVD deposited TiO_2 thin films. 38 of these plates have been sent to Vahterus where they are in the process of being assembled and welded into a heat exchanger unit as illustrated in Figure 14. The remaining two plates are at DTI in case further analysis of the pattern and TiO_2 film will be needed.

Figure 14: Coated plates welded at Vahterus

Prize consideration:

Spray deposition of particles is a low cost technique. For these heat exchanger plates, 14.1 mL acetone and 0.9 mL particle suspension were consumed per plate.

Energy Efficient Heat Exchangers for HVAC Applications   *24*
Project No: 314648 – EnE-HVAC
Report on D4.1: Proof-of-concept

To lower the price of preparing nanostructured surfaces on large areas, a synthesis route for the production of polystyrene nanoparticles with diameters of 500nm have been established dramatically reducing the price of the deposition step compared to currently available particles for commercial use. This synthesis brings the price per kg of raw material down to appr. €70 per kilo vs. €225.000 per kilo for commercially available 500nm PS spheres. These commercially available spheres have a very large price due to their use as calibration standard for size measurements, and hence a very narrow size distribution. The in-house synthesized nanoparticles have a larger size distribution (ranging from 450nm to 530nm), but will be very useful for the purposes in this project.

The equipment needed for spray deposition (an airbrush and a source of pressurized air) is technically simple and cheap making the costs for equipment negligible. In terms of labor, the current setup allows us to manually spray coat a heat exchanger plate in approximately 5 min. For further scale up, it might be profitable to design and make use of a spray deposition machine.

Providing a substantial scaling up of the production, an investment in an inline coater system would be relevant to lower the price of the TiO_2 coatings. Acquiring such a system involves a large investment, though, and the price of coating a single plate will depend strongly on the depreciation allowances. An estimate on the price for coating a heat exchanger plate with TiO_2 is approx. €20.

Sol-gel coatings for heat transfer

The objective of this part of report it is to cover the scale- up of the selected compositions in order to test the behavior of the coatings on corrugated steel plates from Vahterus. This part of the report is the continuation of the tentative cost of the coating process reported previously in D2.3.

Energy Efficient Heat Exchangers for HVAC Applications   *25*
Project No: 314648 – EnE-HVAC
Report on D4.1: Proof-of-concept

Due to the large dimensions of the corrugated plates from Vahterus (Φ=30cm), it has been necessary to modify elements of the synthesis of the sol-gels, and in other cases, it has also been essential to design and manufacture new elements for the application of the sol-gels. The application elements designed for the scale-up process is described below.1. Sol-gel elevator support for substrates. 	2. Substrate support for thermal treatment.
3. Silicon bath with specific dimensions for post-treatment 	4. Reactor for substrate post-treatment
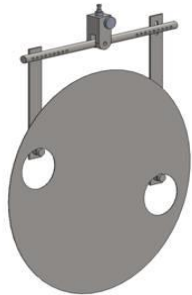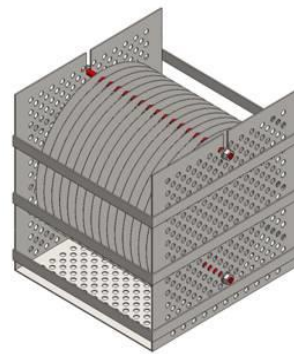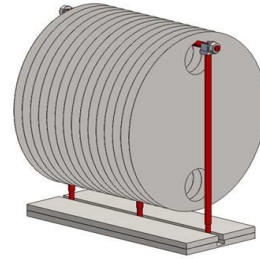
Energy Efficient Heat Exchangers for HVAC Applications
Project No: 314648 – EnE-HVAC
Report on D4.1: Proof-of-concept

26
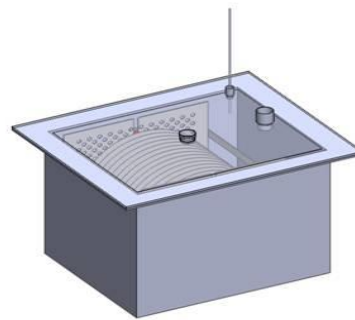
5. Final configuration of post-treatment
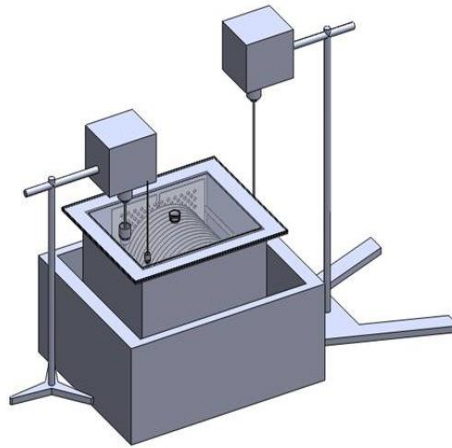
The elements 1 and 2 are needed for Sol-gel coatings without post-treatment (strategy). For post-treatet sol-gels, all of the above elements are needed for the manufacturing process which adds significantly to the manufacturing price when selecting these sol-gels.

Estimating the cost will be an important parameter for the final selection of coatings in case there are several similarly performance coatings. Although the price that we could manage as research centre, of the chemical component needed to develop the coating at large scale, is significantly higher that the real price for industrial production.

Following tables below (

Table 7 and Table 8) shows the estimated cost of scale- up to 60 SS corrugated Vahterus discs, using only a sol-gel process (strategy A) and post-treatment technology (strategy B). The estimations are made for 60 discs from Vahterus. The total surface area (in m^2) used for heat exchanger discs are 0,070m^2 per disc.

Table 7: Estimated cost of strategy A.

STRATEGY A: SOL-GEL SYNTHESIS						
Composition	Nature	CA	Required volume sol-gel (L)	Sol-gel cost (12l)	Cost €/m²	Cost €/Vatherus disc
Composition 1	hidrophobic	106	12	618,72	555,8149186	39,28833333
Composition 2	hidrophobic	91	12	200,05	457,1155061	32,31166667
Composition 3	hidrophobic	103	12	2886,7	1090,668591	77,095
Composition 5	hidrophilic	12	12	618,72	555,8149186	39,28833333
Composition 6	hidrophilic	7	12	200,05	457,1155061	32,31166667

Table 8: Estimated cost of strategy B.

STRATEGY B: POST-TREATMENT						
Composition	Nature	CA	Required volume post-treatment (L)	post-treatment cost (240L)	Cost €/m²	Cost €/Vatherus disc
Composition 4	hidrophobic	109	240	6480	2616,571881	184,955
Composition 7	hidrophobic	118	240	223776	53851,61135	3806,555
Composition 8	hidrophobic	110	240	196080	47321,32247	3344,955
Composition 9	superhidrophobic	121	240	6480	2517,872469	177,9783333
Composition 10	superhidrophobic	123	240	223776	53752,91194	3799,578333
Composition 11	superhidrophobic	125	240	196080	47222,62306	3337,978333

Due to the large volume post-treatment formulation (around 240L) it is necessary to prepare for the 60 SS disc, the price of the post-treatment process is too high. For this reason, a viability study has been performed in order to re-use the volume of post-treatment. For this, it is estimated that four batches (around 60L of solution) of 15 samples are necessaries to perform the post-treatment for all of Vahterus disc (60 SS disc). Table 9 shows the C.A measurements of one sample of the different batches of re-using the post-treatment solution.

Table 9: Contact angles on large scale disks

	CA coating	CA coating post-treatment
Composition 9	91	121
Re-use Tester1	91	119
Re-use Tester2	91	116
Re-use Tester3	91	123
Re-use Tester4	91	117

Energy Efficient Heat Exchangers for HVAC Applications   *29*
Project No: 314648 – EnE-HVAC
Report on D4.1: Proof-of-concept

All the samples show similar values of C.A. independently of the number of batch. So, the re-use of the volume of post-treatment solution has been validated demonstrating that the superhydrophobicity of the samples are not affected.

Table 10 below show the estimated cost of scale- up to 60 SS corrugated Vahterus discs re- using the post-treatment solution.

Table 10: Estimated cost of strategy B re-using the post-treatment solution.

RE-USE VOLUMEN OF POST-TREATMENT						
Composition	Nature	CA	Required volume post-treatment (L)	post-treatment cost (60L)	Cost €/m²	Cost €/Vatherus disc
Composition 4	hidrophobic	109	60	1620	654,1429703	46,23875
Composition 7	hidrophobic	118	60	55944	13462,90284	951,63875
Composition 8	hidrophobic	110	60	49020	11830,33062	836,23875
Composition 9	superhidrophobic	121	60	1620	629,4681172	44,49458333
Composition 10	superhidrophobic	123	60	55944	13438,22798	949,8945833
Composition 11	superhidrophobic	125	60	49020	11805,65576	834,4945833

As a function of the results obtained of contact angle measurements (CA) and DTI test, previously reported in D2.3 of WP2, **composition 1, 4, 6 and 11** has been selected as candidate compositions to scale- up. Consideering parameters such as performance and price, TEK and DTI decided to select **composition 1,** to be deposited onto corrugated heat exchanger disks from Vahterus. The scale-up have been done, as illustrated in the images below.

1:
Corrugated stainless steel disks from Vahterus

2 and 3:
The dip-coating process.

4, 5 and 6:
Substrate support with coated SS disc.

7 and 8:
Substrate support for thermal treatment into the oven.

Energy Efficient Heat Exchangers for HVAC Applications
Project No: 314648 – EnE-HVAC
Report on D4.1: Proof-of-concept

31
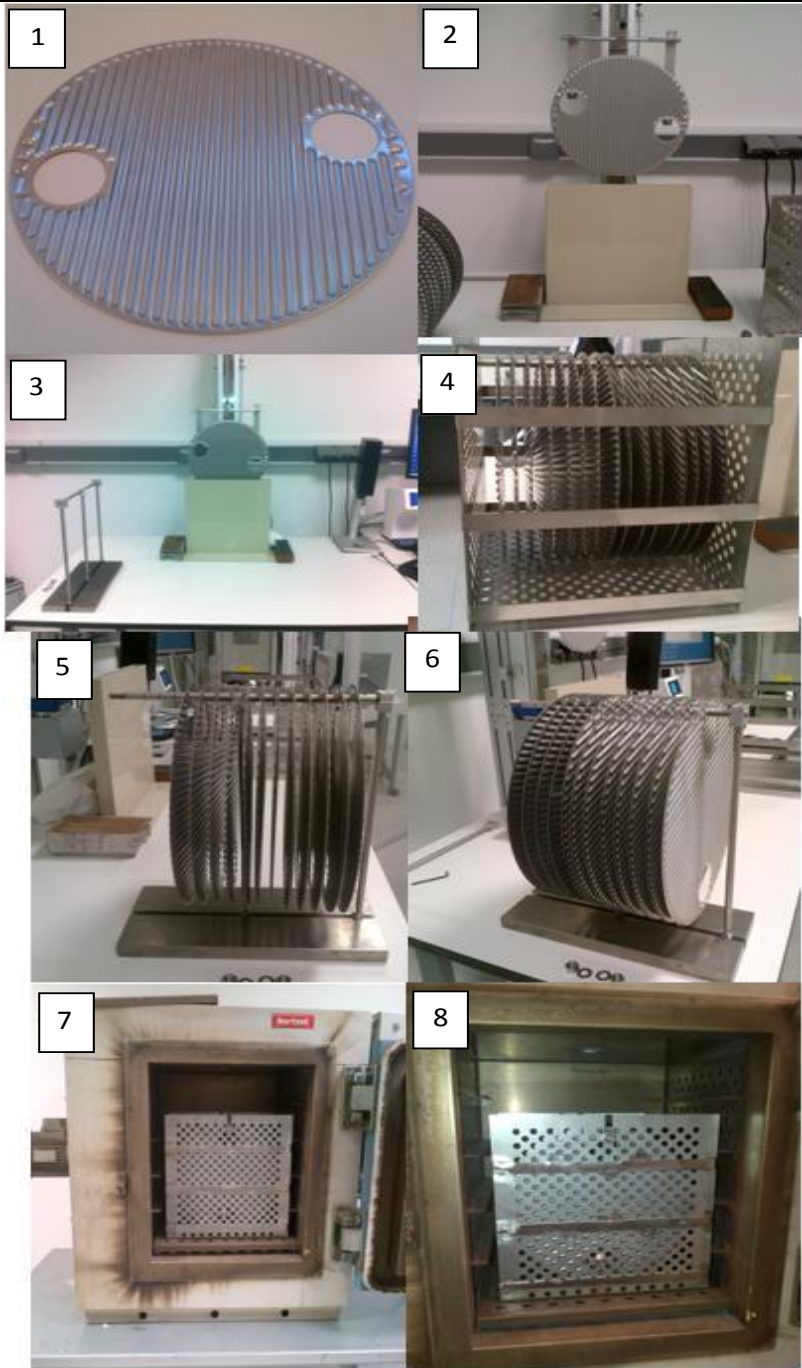
Among the 60 SS discs, 30 samples have been coated on both sides and another 30 samples only on one side. Table 11 below summarizes the C.A measurements of real SS disc, confirming that all the samples are similar between them and there are no differences in hydrophobicity behavior.

Table 11: measurements of Vahterus disc coated with composition 1

	Representative CA coating onto SS Vahterus disc
Batch 1	122.9
Batch 2	122.7
Batch 3	123.5
Batch 4	123.2

These coated heat exchanger disks have been sent to Vahterus to be assembled into final heat exchangers ready for industrial scale tests at the tests laboritories of Vahtererus and DTI for testing for improvements on heat transfer in NH_3 and CO_2.